Experimental Observation of Heaving Motion Effect on CHF in heater rod with axially cosine-shaped power profile

Ja Hyun Ku, Jin-Seong Yoo, Heepyo Hong, Hyukjae Ko, Giwon Bae, Goon-Cherl Park, Hyoung Kyu Cho*
Department of Nuclear Engineering, Seoul National University, 1, Gwanak-ro, Gwanak-gu, Seoul 08826
**Corresponding author: chohk@snu.ac.kr*

***Keywords : Critical heat flux, cosine-shaped power profile, heaving motion, floating nuclear power plant, simulant fluid**

1. Introduction

Floating Nuclear Power Plants (FNPPs) are a type of Nuclear Power Plant that operates in ocean environments and attract attention for their various advantages, such as seawater desalination and providing electricity to areas with limited access [1]. Russia has developed Akademik Lomonosov, equipped with two KLT-40s, which has been in operation since 2019 [2]. In addition to Russia, various countries are developing FNPPs, including OFNP-300 and ThorCon in the US, CMSR in Denmark, and BANDI in South Korea [3-6].

In the ocean environment, the reactor is constantly affected by external forces, which affect its thermal-hydraulic behavior. Among them, CHF can also be affected by the motion conditions, which is essential for nuclear safety. Recently, Seoul National University conducted experiments under rolling and heaving conditions using a bare rod with a uniform power profile and a helical rod with a uniform power profile to investigate the effect of ocean motion on CHF [7-10]. However, in actual reactor operation, the nuclear fuel rods have an axially cosine-shaped power profile, so it is necessary to conduct experiments using heater rods with such a power profile. Therefore, there is a need for more studies and data on CHF experiments that simulate an axially cosine-shaped power profile under motion conditions.

In this study, the CHF experiment was conducted using a heater rod with an axially cosine-shaped power profile under heaving conditions. The motion platform, NEOUL-H, was utilized to simulate sinusoidal heaving motion, and the annulus test section with a single heater rod was used. In addition, R134a was selected as the working fluid to simulate the high-pressure experimental conditions of PWR using water as the working fluid. The experimental results showed that the CHF under the heaving condition decreased compared to the vertical static condition. The parametric trend of the heaving motion effect was also confirmed.

2. Experimental facility

2.1. Heaving motion platform, NEOUL-H

NEOUL-H is a platform designed to simulate heaving motion, which can perform CHF experiments under vertical static and heaving conditions. The main design parameters are acceleration and period. When the heaving motion is given by Eq. (1), the heaving acceleration can be calculated as Eq. (2).

(1) $A(t) = A_m \sin\left(\frac{2\pi}{T}t\right)$

(2) $a(t) = -A_m \frac{4\pi^2}{T^2} \sin\left(\frac{2\pi}{T}t\right)$

where A, A_m, T, and a are the displacement of the test loop, amplitude of heaving motion, heaving period, and heaving acceleration, respectively.

NEOUL-H has maximum acceleration of 0.6g, and minimum period of 3 s, which were determined based on the data in the open literature [11-13].

In this experiment, both vertical static and heaving conditions tests were performed for each thermal-hydraulic condition to confirm the heaving motion effect. The heaving motion conditions can be found in Table I.

Table I: Heaving conditions

Acceleration magnitude [g]	Amplitude [mm]	Period [s]
0.2	1400	5.31
	700	3.75
	450	3.01
0.4	1400	3.75
	900	3.01
0.6	1400	3.06

2.2. Test Loop and CHF test conditions

The test section has annulus geometry with single heater rod, as shown in Fig. 1. The CHF test loop uses R134a as working fluid to simulate PWR operating pressure conditions under low pressure. Based on fluid-to-fluid scaling criteria [7], experimental conditions were set as shown in Table II. The heater has axially cosine-shaped power profile, so the CHF is expected to occur at the different axial positions depending on the experimental conditions. Therefore, 8 thermocouples were installed on the heater rod to measure wall temperature at different axial locations, as depicted in Fig. 1. The power input of the heater was increased stepwise by less than 1% of the current heater power input until the CHF occurrence to reduce uncertainty in the experiment due to steps in the power increase. When the sudden rise of the wall temperature occurs, it indicates that the CHF has occurred, so the power input is reduced by the operator. The thermal-hydraulics conditions, such as outlet pressure, inlet temperature, and mass flux were maintained nearly constant value under heaving condition, minimizing the effect of other phenomena, such as flow oscillations.

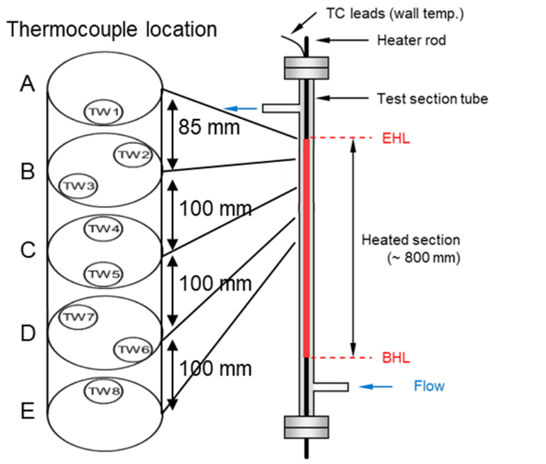

Fig. 1. Schematic diagram of test section and location of thermocouples

Table II: CHF test conditions

Parameters	R134a test condition	Water equivalent condition
Outlet pressure [MPa]	1.6 ~ 3.2	10 ~ 18
Inlet mass flux [kg/m^{2}s]	90 ~ 1750	140 ~ 2350
Inlet subcooling [K]	8 ~ 43	21 ~ 117

3. Experimental results

In this study, CHF is defined as the heat flux at which the wall temperature excursion occurs, and the wall temperature continues to rise until the power is cut off. As mentioned earlier, the heater used in this experiment has an axially cosine-shaped power profile, and thermocouples were installed along the axial direction. CHF is detected through the thermocouple response, but since the thermocouples are spaced from a minimum of 15 mm to a maximum of 100 mm apart, it is not reasonable to assume that the thermocouple showing the temperature excursion is the exact location of the CHF occurrence. Therefore, for the same heater power, the heat flux varies significantly depending on the axial position, so we used the average heat flux rather than the localized heat flux in our analysis.

3.1. CHF under vertical static conditions

As shown in Fig. 2, the test results are classified based on Katto's CHF regime map and critical quality obtained from the experiment. The classification of experimental results confirms that the CHF experiment was conducted for dryout and DNB cases. The dryout phenomena were observed under low mass flux conditions. As shown in Fig. 3, with a slight increase in power input, temperature rise occurs at the specific location of the heater (location A in Fig. 3). After the stabilization of the temperature rise, in the further power step, temperature excursion occurs at the other location of the heater (location B in Fig. 3).

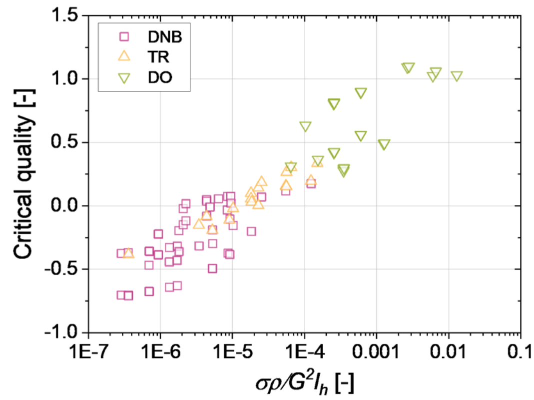

Fig. 2. Classification of experimental results into CHF regime map

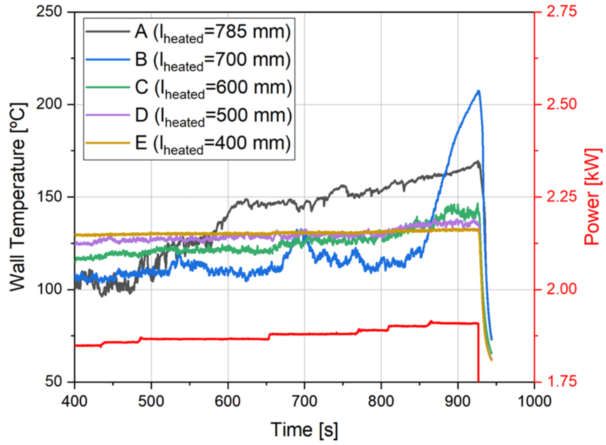

Fig. 3. Wall temperature response of heater rod for dryout case under vertical static condition (P=1.6 MPa, G=90 kg/m^{2}s, T_{sub}=8 K)

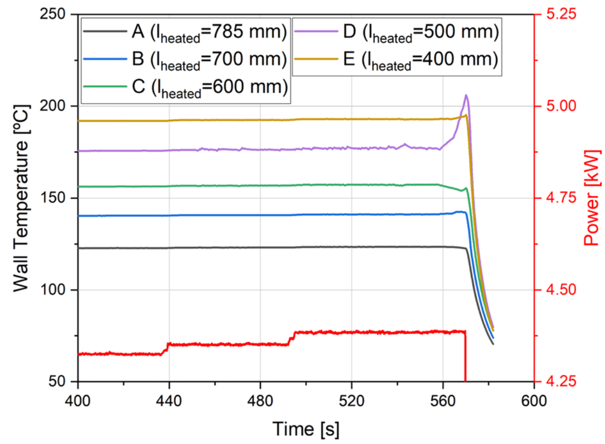

Fig. 4. Wall temperature response of heater rod for DNB case under vertical static condition (P=2.5 MPa, G=1509 kg/m^{2}s, T_{sub}=23 K)

On the other hand, the DNB phenomena were observed under high mass flux conditions, and the location of CHF occurrence was closer to the center of the heater. As shown in Fig. 4, with increasing power, the rapid temperature excursion occurs at a specific location (location D in Fig. 4). The location where DNB-type CHF occurred was mostly right after the center of the heater.

3.2. CHF under heaving conditions

We investigated the parametric effect of heaving motion on CHF, as shown in Fig. 5 and 6. In each figure, the y-axis is the CHF ratio between the vertical static and heaving conditions. A y-value greater than 1 indicates an increase in CHF in the heaving condition compared to the vertical static condition. On the other hand, a y-value less than 1 indicates a decrease in CHF in the heaving condition compared to the vertical static condition. In most cases, CHF decreased due to heaving motion. Previous research has explained the decrease in CHF due to heaving motion as a reduction in net gravity.

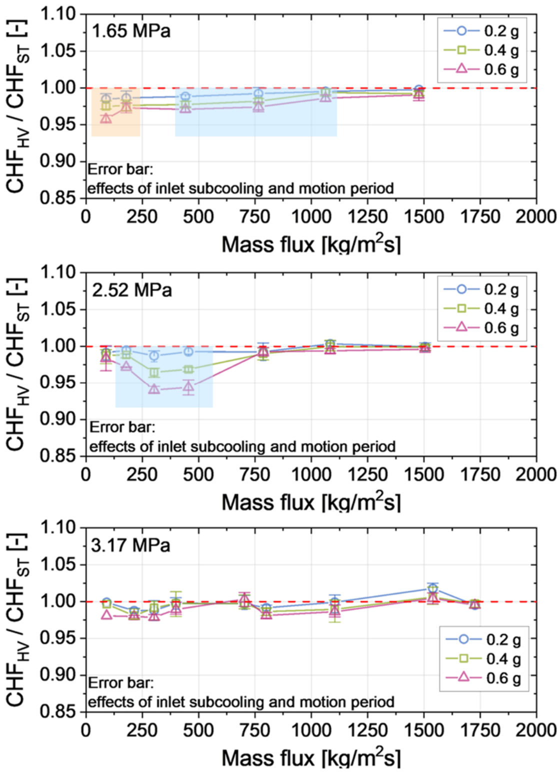

Fig. 5. Parametric effect of heaving motion on CHF: mass flux

Near the critical quality of 0 (blue color box in Fig. 5 and 6), the decrease in net gravity reduces relative velocity between phases, promoting the formation of large vapors and developing early CHF.

On the other hand, at a critical quality above 0.6 (orange color box in Fig. 5 and 6), the decrease in net gravity reduces the relative velocity difference between phases, leading to increased vapor superheating and reduced interfacial heat transfer. This results in a thinner liquid film, leading to the early development of dry patches.

However, no clear trend was observed at critical qualities below 0, and no significant temperature oscillations were observed before CHF occurred in the experimental conditions belonging to the high mass flux DNB. Thus, it was concluded that heaving motion does not significantly affect CHF under these experimental conditions.

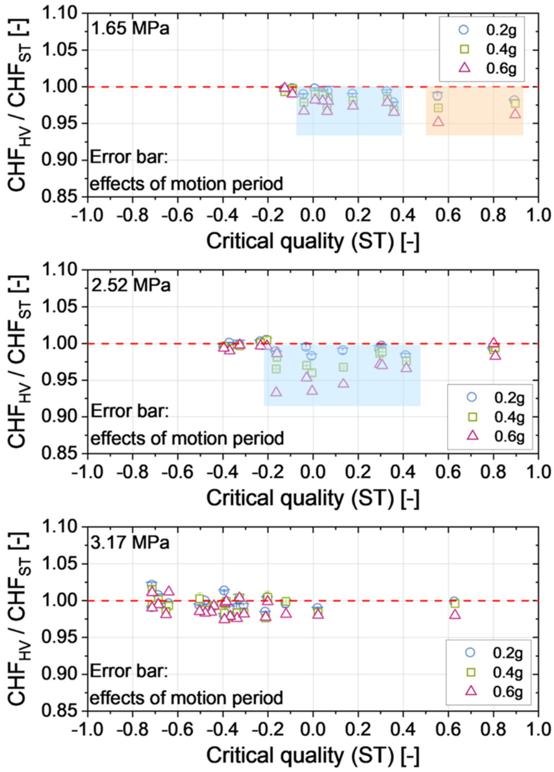

Fig. 6. Parametric effect of heaving motion on CHF: critical quality

4. Conclusion

In this study, CHF experiments were conducted under heaving conditions with an annulus test section using a heater rod with an axially cosine-shaped power profile. The test loop using R134a was constructed to simulate PWR's high-pressure water conditions, and the heater surface temperature was monitored through eight thermocouples located in the heater at axially different locations. The temperature trends in different CHF regimes, dryout and DNB, were analyzed. In addition, it was confirmed that in most cases, the heaving motion reduced CHF. The parametric effects of heaving motion on CHF according to the CHF regime were investigated. Except for the high mass flux DNB case, it was confirmed that the reduction in net gravity leads to an earlier onset of CHF.

Currently, experimental results are being analyzed using thermocouple locations where CHF occurs. Conducting such analysis will provide further insight into the effects of heaving motion in this CHF experiment with an axially cosine-shaped power profile.

REFERENCES

[1] Kostin, V. I., Panov, Y. K., Polunichev, V. I., & Shamanin, I. E. "Floating power-generating unit with a KLT-40S reactor system for desalinating sea water." Atomic Energy, 102.1 (2007): 31-35.
[2] Belyaev, V. M., et al. "The world's first floating NPP: Origination and direction of future development." Atomic Energy 129.1 (2020): 27-34.
[3] Buongiorno, J., et al. "The offshore floating nuclear plant concept." Nuclear Technology 194.1 (2016): 1-14.
[4] Jorgensen, Lars, and Robert Hargraves. "ThorCon reactor." Molten Salt Reactors and Thorium Energy. Woodhead Publishing, 2024. 835-845.
[5] Pater, Mateusz, Jonas Stampe, and Eirik Eide Pettersen. "Nuclear reactor barge for sustainable energy production." WCFS2020: Proceedings of the Second World Conference on Floating Solutions, Rotterdam. Springer Singapore, 2022.
[6] Kang, Han Ok, Byung Jin Lee, and Sang Gyu Lim. "Light water SMR development status in Korea." Nuclear Engineering and Design 419 (2024): 112966.
[7] Kim, Geon-Woo, et al. "Critical heat flux characteristics of flow boiling on a heater rod under inclined and rolling conditions." International Journal of Heat and Mass Transfer 189 (2022): 122670.
[8] Lee, Chang Won, et al. "Experimental investigation of helical fin and inclination effect on critical heat flux." International Journal of Heat and Mass Transfer 215 (2023): 124482.
[9] Yoo, Jin-Seong, et al. "Experimental study on flow boiling CHF in annulus channel under heaving conditions using simulant fluid R134a targeting nuclear reactor applications." Applied Thermal Engineering 236 (2024): 121906.
[10] Yoo, Jin-Seong, et al. "Experimental study on flow boiling CHF of a helical finned rod under heaving conditions using simulant fluid R134a." International Journal of Heat and Mass Transfer 232 (2024): 125927.
[11] Otsuji, Tomoo, and Akira Kurosawa. "Critical heat flux of forced convection boiling in an oscillating acceleration field—I. General trends." Nuclear Engineering and Design 71.1 (1982): 15-26.
[12] Isshiki, Naotsugu. "Effects of heaving and listing upon thermo-hydraulic performance and critical heat flux of water-cooled marine reactors." Nuclear engineering and Design 4.2 (1966): 138-162.
[13] Lewis, Edward V. "Principles of naval architecture." Motions in waves and controllability (1989): 126-136.